ADVANCES IN ATMOSPHERIC SCIENCES, VOL. 24, NO. 1, 2007, 147–151

The Generalized Energy Equation and Instability in the Two-layer Barotropic Vortex

ZHANG Ming* (张 铭), ZHAO Yanling (赵艳玲), HUANG Hong (黄 泓), and LIANG Danqing (梁丹青)

The Laboratory of Atmospheric Circulation and Short-range Climatological Forecasting, Institute of Meteorology, PLA University of Science and Technology, Nanjing 211101

(Received 26 January 2006; revised 15 June 2006)

ABSTRACT

The linear two-layer barotropic primitive equations in cylindrical coordinates are used to derive a generalized energy equation, which is subsequently applied to explain the instability of the spiral wave in the model. In the two-layer model, there are not only the generalized barotropic instability and the super high-speed instability, but also some other new instabilities, which fall into the range of the Kelvin-Helmholtz instability and the generalized baroclinic instability, when the upper and lower basic flows are different. They are perhaps the mechanisms of the generation of spiral cloud bands in tropical cyclones as well.

Key words: two-layer barotropic vortex, generalized energy equation, instability, spiral wave

DOI: 10.1007/s00376-007-0147-1

1. Introduction

Tropical cyclones, a sort of violent storm taking place over tropical oceans, have received lots of attention by scientists as one of the most serious natural disasters, and much valuable progress has been achieved in the relevant research (Chen and Meng, 2001; Meng et al., 2002; Chen and Luo, 2004; Chen et al., 2004). The spiral cloud and rain bands developing with the eye-wall of typhoons/hurricanes are called spiral cloud bands, which have been the subject of observational studies for a long time (Wexler, 1947; Ligda, 1955; Senn and Hiser, 1959; Kurihara, 1976; Guinn and Schubert, 1993; Liu et al., 1997; Nasuno and Yamasaki, 2001; Liu et al., 1999; Yu, 2002; Chow et al., 2002). On the basis of observations of Ligda (1955), it is found that the spiral cloud bands, whose translational speeds are higher than wind speeds commonly, move along the air flow and around eyes of tropical cyclones. In the observation data of weather surveillance radars in Senn and Hiser (1959), it is further reflected that spiral bands spread outward and the life time of a single spiral band is 1–2 hours. The feature of large-scale spiral bands reflected in a whole mature tropical cyclone is the primary knowledge that we have on spiral bands of tropical cyclones. Gray (1968) considered that, in a tropical cyclone, there are azimuthal symmetry flows and asymmetry flows. The latter is usually the most distinct part in radar and satellite pictures and spiral bands are the representation of it. Based on radar observations, Diercks and Anthes (1976a, b) pointed out that spiral bands, of which the angular velocity is usually greater than that of the basic flow, are distributed in order and move around the centers of tropical cyclones. Furthermore, spiral bands move outward along the radial direction at a speed of about 28 m s^{-1}, which is approximately the spread velocity of gravity waves. Moreover, trailing spiral bands typically appear in the Northern Hemisphere and their azimuths vary from 2 to 4. The spaces between two adjacent bands are often as wide as scores of kilometers to several hundred kilometers while those near centers are even wider. Guinn and Schubert (1993) further pointed out that there are two kinds of spiral bands in tropical cyclones, viz. internal spiral bands and external spiral bands. The former are in the neighborhood of centers of vortexes, which are evidently reflected by radar echoes but indistinct in the satellite pictures due to the coverage of cirrus clouds. The latter, which are probably long and narrow, generally lie in the region 500 km away from the center of the typhoon. Both the rain bands and the air near cores rotate around the centers of tropical cyclones, while a great deal of air in the external re-

*E-mail: gq068@jlonline.com

gion moves through them. In order to find features of micro-scale spiral bands observed in tropical cyclones, Tuttle and Gall (1995) studied the radar reflectivity field with the wave train analysis technique. After he analyzed the radar data of three strong typhoons, Gall et al. (1998) pointed out that microscale spiral bands frequently exist within 100 km of the center. They are originally 10 km in width, and can extend to 100 km when rotated clockwise outward around the typhoon at a speed close to the tangential wind speed. Their potential vorticity are high in high reflectivity regions, leading to changes of at least 8 m s^{-1} in wind speed. Through observing the two-way airborne radar, Reasor et al. (2000) pointed out that the microscale structure of spiral bands is on the outer side of the high vorticity region in the radial direction, with the magnitude of the radial wave length being 5–10 km. Barnes et al. (1991) and May (1996) suggested that spiral bands are composed of orderly strong convection cells under the background of wide cumulostratus rain, and some rotate around the center and propagate radially. Thus it shows that the spread velocity of the microscale spiral bands which are 5–10 km in the radial and tangential directions away from the cyclone centers is not consistent. Perhaps they actually spread outward and counterclockwise at different speeds. Although the function of these microscale spiral bands in the tropical cyclone dynamics has not been made clear yet, it is not difficult to draw the following conclusions about their essence from the above observation. First, the rotation velocity of spiral bands around the eye of a tropical cyclone is unequal to that of air flow, which indicates that they are a substantial belt composed of different air particles. Secondly, they tend to grow in the radial direction, which indicates that radial energy propagation is taking place. So it can be hypothesized that the spiral band is a kind of wave in typhoons, which can be called a spiral wave, and its cause can be ascribed to the instability of the basic flow in a vortex. The instabilities of barotropic vortexes have been studied before (Huang and Zhang, 2003). However, it is more suitable to study the instability of the basic flow in them, for the real atmosphere is baroclinic. Due to the complexity of the problem, first, a two-layer barotropic fluid is used to approach the baroclinic fluid, which is significant to the understanding of the occurrence and evolution of spiral cloud bands in tropical cyclones.

2. Mathematical model

It is well known that it is not only convenient but also feasible to adopt a multilayer barotropic model to approach a baroclinic model. Zeng (1979) even gave the control equations of the multilayer barotropic model, of which, the simplest one is a two-layer barotropic model. Therefore, the barotropic primitive equations of the two-layer homogeneous fluid in cylindrical coordinates (Liang and Zhang, 2003) are adopted to derive linear equations, setting:

$$u_k = u'_k, \quad v_k = \overline{V}_k(r) + v'_k,$$
$$\Phi_k = gh_k = g\overline{H}_k(r) + gh'_k = \overline{\Phi}_k + \Phi'_k \,. \tag{1}$$

Here, the subscript $k = 1, 2$, which is also used infra. Omitting the symbol "$'$ ", the control equations are given as:

$$\left(\frac{\partial}{\partial t} + \frac{\overline{V}_k}{r}\frac{\partial}{\partial \theta}\right) u_k - \tilde{f}_k v_k = -\frac{\partial(a_k\Phi_1 + \Phi_2)}{\partial r} \,, \tag{2-1}$$

$$\left(\frac{\partial}{\partial t} + \frac{\overline{V}_k}{r}\frac{\partial}{\partial \theta}\right) v_k - \tilde{f}_k u_k = -\frac{\partial(a_k\Phi_1 + \Phi_2)}{r\partial \theta} \,, \tag{2-2}$$

$$\left(\frac{\partial}{\partial t} + \frac{\overline{V}_k}{r}\frac{\partial}{\partial \theta}\right) \Phi_k + C_{0k}^2\left(\frac{1}{r}\frac{\partial r u_k}{\partial r} + \frac{1}{r}\frac{\partial v_k}{\partial \theta}\right) + u_k\frac{dC_{0k}^2}{dr} = 0, \tag{2-3}$$

where, $\tilde{f}_k = f + 2\overline{V}_k/r$, $\hat{f}_k = f + \overline{V}_k/r + d\overline{V}_k/dr$, $C_{0k}^2 = \overline{\Phi}_k$; $a_1 = 1, a_2 = \rho_1/\rho_2$, and the positive constant a_2 represents the ratio of density between the upper level and the lower level respectively. The boundary conditions are:

$$u_1|_{r=0} = 0 \;\; u_1|_{r=\tilde{r}} = 0 \,, \tag{3-1}$$

$$u_2|_{r=0} = 0 \;\; u_2|_{r=\tilde{r}} = 0 \,, \tag{3-2}$$

where $\tilde{r}$ is the radius of the two-layer barotropic vortex.

In order to derive the energy equation, we make $C_{0k}^2 u_k \cdot$(2–1)$+C_{0k}^2 v_k \cdot$(2–2)$+\Phi_k \cdot$(2–3). Then the result is integrated over the horizontal range S. The range of radius r is $[0, \tilde{r}]$ and that of azimuth θ is $[0, 2\pi]$, thus the energy equations at upper and lower levels are derived. Following the means in Zeng (1979), the generalized energy equation at upper and lower levels can be obtained. Then the upper-level generalized equation is multiplied by a_2 and added to the lower-level generalized equation. Finally, the generalized energy equation of the two-layer model can be derived as:

$$\frac{\partial}{\partial t}\iint\limits_S \left\{\sum_{k=1}^{2} b_k\frac{C_{0k}^2}{2}\left[\left(1 - \frac{\overline{V}_k^2}{C_{0k}^2}\right)v_k^2 + u_k^2 + \left(\frac{\Phi_k + \overline{V}_k v_k}{C_{0k}}\right)^2 - \frac{\overline{V}_k}{F_k}\Omega_k^2\right] + a_2\Phi_1\Phi_2\right\} r dr d\theta = 0 \,, \tag{4}$$

where

$$b_1 = a_2 > 0, b_2 = a_1 > 0,$$
$$\Omega_k = \left(\frac{\partial r v_k}{r\partial r} - \frac{u_k}{r\partial\theta}\right) - \left(f + \frac{dr\overline{V}_k}{rdr}\right)\frac{\Phi_k}{C_{0k}^2},$$
$$F = -C_{0k}^2\frac{d\tilde{\Omega}_k}{dr},$$

and

$$\tilde{\Omega}_k = \left(f + \frac{dr\overline{V}_k}{rdr}\right)\frac{1}{C_{0k}^2}$$

is the absolute vorticity of the basic flow.

3. Discussion

3.1 *Instability criterion*

The following equation can be obtained from (4):

$$\iint_S \left\{\sum_{k=1}^{2} b_k \frac{C_{0k}^2}{2}\left[\left(1-\frac{\overline{V}_k^2}{C_{0k}^2}\right)v_k^2 + u_k^2 + \left(\frac{\Phi_k + \overline{V}_k v_k}{C_{0k}}\right)^2 - \frac{\overline{V}_k}{F_k}\Omega_k^2\right] + a_2\Phi_1\Phi_2\right\} rdrd\theta = \text{Const.} \quad (5)$$

Equation (5) indicates that, if $1 - \overline{V}_k^2/C_{0k}^2 > 0$, then $\overline{V}_k/F_k < 0$ and $\Phi_1\Phi_2 > 0$ can apply to every place in region S, the generalized energy of the two-layer barotropic model is finite and the disturbance is stable at any time. Thus the necessary conditions of the instability of the disturbance are:

$$\overline{V}_k^2 > C_{0k}^2 \quad (6\text{-}1)$$
$$\overline{V}_k/F_k > 0 \quad (6\text{-}2)$$
$$\Phi_1\Phi_2 < 0\,. \quad (6\text{-}3)$$

Equations (6-1) and (6-2) are the criteria of the super high-speed instability and the generalized barotropic instability respectively, which has been discussed in Zeng (1979). However, in the two-layer barotropic model, the instability criteria are also linked to $\Phi_1\Phi_2$, namely the interaction between the upper-layer and the lower-layer liquid. It is noticed that the variables in Eqs. (6-1) and (6-2) are all basic fields, while the variables in Eq. (6-3) are a disturbed field. If $\Phi_1\Phi_2 < 0$, namely, if the upper and lower disturbance thickness fields are in opposite phase, then there will be instability in the model. The numerical calculation (Liang and Zhang, 2003) indicates that the upper-layer and the lower-layer thickness fields are indeed in opposite phase when there is instability, which is consistent with the conclusions in this paper.

3.2 *Discussion*

The two-layer barotropic model in cylindrical coordinates is used in this paper. There is tangential basic flow complying with gradient wind balance at both upper and lower layers. If the curvature of cylindrical coordinates is ignored, the gradient wind balance transforms into geostrophic balance. It is well known that the flow is always unstable as long as the upper-layer and the lower-layer basic flows are different, if the Coriolis force is ignored, which is called Kelvin-Helmholtz instability (Thomson, 1871). On the other hand, the instability of a two-layer quasi-geostrophic model have been studied by Phillips (1954), whose results show that instability called the baroclinic instability of the Rossby wave may occur when the upper-layer and the lower-layer basic flows are different. However, they can only be considered as special cases of the model used in this paper which is more complex compared with those in the two previous cases. The Coriolis force and the curvature of cylindrical coordinates are ignored in the former, whereas the cylindrical coordinates are ignored while the geostrophic basic flow is adopted in the latter. Therefore the instability corresponding to Eq. (6-3) includes both Kelvin-Helmholtz instability and the baroclinic instability. As to the latter, it is better to call it generalized baroclinic instability, for the instability disturbance is a geostrophic vortex wave. Therefore, as long as Eq. (6-3) is obeyed, there may be two instabilities in this model, which results in the generation of a spiral wave.

Finally, the instability in the two-layer barotropic model is discussed in detail, in which the radial wind profile (Liang and Zhang, 2003) (Fig. 1) is adopted:

$$\overline{V}_k = V_{\max k}(r/r_{\max k})\exp[0.5(1 - r^2/r_{\max k}^2)], \quad k = 1, 2. \quad (7)$$

In the profile, $V_{\max k}$ is the maximum wind speed at the upper or lower layer, $r_{\max k}$ is the radius of maximum wind speed at the upper or lower layer, and $V_{\max 1} = 10$ m s^{-1}, $V_{\max 2} = 35$ m s^{-1}. The maximum wind speed radius at the upper level is the same as that at the lower level, that is $r_{\max k}$=62.5 km. The static thickness of the fluid at the upper and lower layers are both 3 km. So that real tropical cyclones can be simulated better, the horizontal radius is set to be $\tilde{r} = 500$ km in the computation region, and the variation curves of C_{0k} and F_k are shown in Fig. 2 and Fig. 3.

Figures 1, 2 and 3 show that $\overline{V}_k$ are always smaller than C_{0k} in the whole region S, which indicates that the criterion in Eq. (6-1) cannot be applied here, namely, there is no super high-speed instability. At a range of less than 125 km from the vortex center, F_k are always positive. So the criterion in Eq. (6-2) is

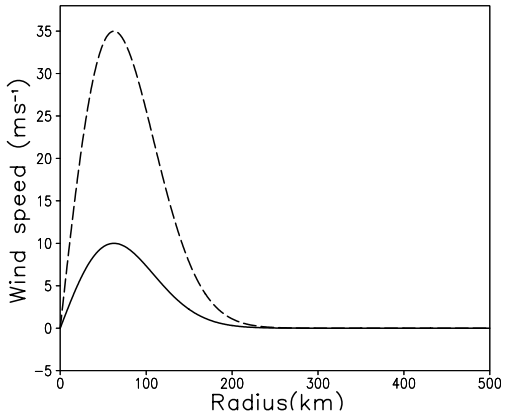

Fig. 1. The radial wind profiles at the upper and lower levels. Solid line represents the upper radial wind profile. Dashed line represents the lower radial wind profile.

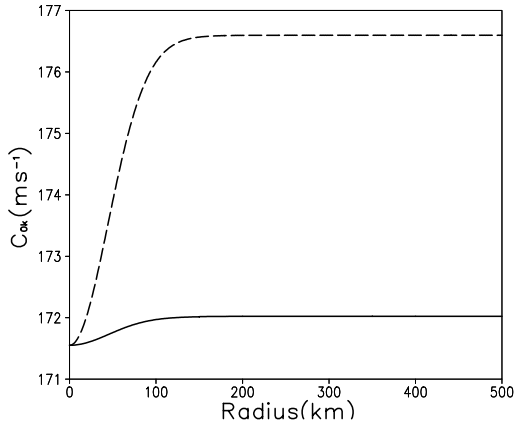

Fig. 2. Distribution of C_{01} and C_{02}. Solid line represents C_{01}. Dashed line represents C_{02}.

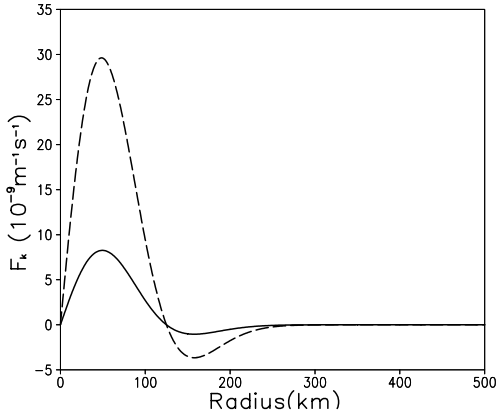

Fig. 3. Distribution of F_1 and F_2. Solid line represents F_1. Dashed line represents F_2.

obeyed here, which indicates that there may be generalized barotropic instability. On the basis of numerical calculation (Liang and Zhang, 2003), it can be learned that there is a mode in which the upper and lower disturbance thickness fields are in opposite phase with the distribution of the radial wind profile mentioned above. Moreover, this mode is unstable. So there are Kelvin-Helmholtz instability and the generalized baroclinic instability, which are caused by different basic flows in the vertical direction. This is also the main difference between the two-layer barotropic model and a general barotropic model.

4. Conclusions

The instability of the linear two-layer barotropic model is studied with the energy method. With the analysis of the generalized energy equation, it can be learned that besides the super high-speed instability and the generalized barotropic instability, the difference between the upper-layer and the lower-layer basic flows also produces other instabilities. For the evident vertical wind shear, the instabilities are found frequently in real tropical cyclones, falling into the range of Kelvin-Helmholtz instability and the generalized baroclinic instability. Because the scales of maximum instability wavelength of Kelvin-Helmholtz instability and the generalized baroclinic instability are different, that is, the former is smaller while the latter is larger, there should be two unstable spiral waves of different scales in our model, which probably correspond to spiral bands of different scales in real tropical cyclones. The theoretical study in this paper can only provide instability types in the model but no material growth rates or scales of the instability mode. Therefore, there is plenty of work needing to be done before applying the conclusions drawn in this paper to studying the occurrence of real spiral cloud bands. Moreover, the release of latent heat of condensation in cumulus convection, which is important in a tropical cyclone, is not considered in our model. That is also a limitation of the two-layer model which will be discussed in our future work.

Acknowledgements. This work was jointly supported by the National Natural Science Foundation of China under Grant Nos. 40575023 and 40175014.

REFERENCES

Barnes, G. M., J. F. Gamache, and G. S. Stossmeister, 1991: A convective cell in a hurricane rainband. *Mon. Wea. Rev.*, **119**, 776–794.

Chen Lianshou, and Meng Zhiyong, 2001: An overview on tropical cyclone research progress in China dur-

ing the past ten years. *Chinese J. Atmos. Sci.*, **25**(3), 420–432. (in Chinese)

Chen Lianshou, Luo Huibang, Duan Yihong, and Yu Hui, 2004: An overview of tropical cyclone and tropical meteorology research progress. *Adv. Atmos. Sci.*, **21**(3), 505–514.

Chen Lianshou, and Luo Zhexian, 2004: Interaction of typhoon and mesoscale vortex. *Adv. Atmos. Sci.*, **21**(4), 515–528.

Chow, K. C., K. L. Chan, and A. K. H. Lau, 2002: Generation of moving spiral bands in tropical cyclones. *J. Atmos. Sci.*, **59**, 2930–2950.

Diercks, J. W., and R. A. Anthes, 1976a: Study of spiral bands in a linear model of a cyclone vortex. *J. Atmos. Sci.*, **33**, 1714–1729.

Diercks, J. W., and R. A. Anthes, 1976b: Diagnostic studies of spiral rain bands in a nonlinear hurricane model. *J. Atmos. Sci.*, **33**, 959–975.

Gall, R., J. Tuttle, and P. Hildebrand, 1998: Small-scale spiral bands observed in hurricanes Andrew, Hugo, and Erin. *Mon. Wea. Rev.*, **126**, 1749–1766.

Gray, W. M., 1968: Global view of the origin of tropical disturbances and storms. *Mon. Wea. Rev.*, **96**, 669–700.

Guinn, T. A., and W. H. Schubert, 1993: Hurricane spiral bands. *J. Atmos. Sci.*, **50**, 3380–3403.

Huang Hong, and Zhang Ming, 2003: Study on destabilization of spiral wave in barotropic vortex. *Journal of Tropical Meteorology*, **19**(2), 197–202. (in Chinese)

Kurihara, Yoshio, 1976: On the development of spiral bands in a tropical cyclone. *J. Atmos. Sci.*, **33**, 940–957.

Liang Danqing, and Zhang Ming, 2003: The spiral wave's instability in vortex of two-layer barotropic fluid. *Journal of Tropical Meteorology*, **19**(4), 405–412. (in Chinese)

Ligda, M. G. H., 1955: Hurricane squall lines. *Bull. Amer. Meteor. Soc.*, **36**, 340–342.

Liu, Y., D.-L. Zhang, and M. K. Yau, 1997: A multiscale numerical study of hurricane Andrew (1992). Part I: Explicit simulation and verification. *Mon. Wea. Rev.*, **125**, 3072–3093.

Liu, Y., D.-L. Zhang, and M. K. Yau, 1999: A multiscale numerical study of hurricane Andrew (1992). Part II: Kinematics and inner-core structures. *Mon. Wea. Rev.*, **127**, 2597–2616.

May, P. T., 1996: The organization of convection in the rainbands of tropical cyclone Laurence. *Mon. Wea. Rev.*, **124**, 807–815.

Meng Zhiyong, Chen Lianshou, and Xu Xiangde, 2002: Recent progress on tropical cyclone research in China. *Adv. Atmos. Sci.*, **19**, 103–110.

Nasuno, T., and M. Yamasaki, 2001: A representation of cumulus-scale effects in a mesoscale-convection-resolving model for tropical cyclones. *J. Meteor. Soc. Japan*, **79**, 1035–1057.

Phillips, N. A., 1954: Energy transformation and meridional circulations associated with simple baroclinic waves in a two-level quasi-geostrophic model. *Tellus*, **6**, 273–286.

Reasor, P. D., M. T. Montgomery, F. D. Marks, and J. F. Gamache, 2000: Low-wavenumber structure and evolution of the hurricane inner core observed by airborne dual-Doppler radar. *Mon. Wea. Rev.*, **128**(6), 1653–1680.

Senn, H. V., and H. Hiser, 1959: On the origin of hurricane spiral rainbands. *J. Meteor.*, **16**, 419–426.

Thomson, W.(Lord Kelvin), 1871: Hydrokinetic solutions and observations. *Phil. Mag.(4)*, **42**, 362–377. Also Kelvin, and Lord, 1910: *Mathematical and Physical Papers (IV)*. Cambridge University Press, Cambridge, 69–85.

Tuttle, J. D., and R. L. Gall, 1995: Radar analysis of Hurricane Andrew and Hugo. *Preprints, 21st Conf. on Hurricane and Tropical Meteorology*, Miami, FL, Amer. Meteor. Soc, 608–610.

Wexler, H., 1947: Structure of hurricanes as determined by radar. *Annals of New York Academy of Sciences*, **48**, 821–844.

Yu Zhihao, 2002: The spiral rain bands of tropical cyclone and vortex Rossby waves. *Acta Meteorologica Sinica*, **60**, 502–507.

Zeng Qingcun, 1979: *Mathematical and Physical Basis of Numerical Weather Forecasting* (*I*). Science Press, Beijing, 230–234. (in Chinese)